R E S E A R C H A R T I C L E

Trends in Biotechnology and
Plant Sciences

USS

Efficient Removal of Lead and Arsenic from Groundwater Using Thiourea-Modified Biochar and Nano Zerovalent Zinc

Sidra Chaudary[1] and Hafsa[2]

1Department of Botany, University of Agriculture, Faisalabad, Pakistan
2Department of Plant Breeding and Genetics, University of Agriculture, Faisalabad, Pakistan

Correspondence
iamhafsa9832@gmail.com

Groundwater contamination by heavy metals such as lead (Pb) and arsenic (As) is a critical environmental and public health issue due to their toxicity and persistence. This study investigates a sustainable and low-cost approach using rice husk-derived biochar modified with thiourea (TMBC) and combined with nano zerovalent zinc (nZVZn) to enhance removal efficiency through adsorption and redox reactions. Batch experiments assessed the effect of pH (3–9), contact time (5–180 min), adsorbent dosage (0.05–0.5 g), and initial metal concentration (10–100 mg/L) on removal performance. The nZVZn–TMBC composite achieved over 90% Pb and 85% As removal at optimal pH values of 5 and 6–7, respectively, reaching equilibrium within 90 minutes. Adsorption followed Langmuir isotherm behavior, indicating monolayer coverage, and pseudo-second-order kinetics suggested chemisorption as the dominant mechanism. Material characterization confirmed successful thiourea functionalization and uniform nZVZn deposition, providing increased surface area (215 m²/g) and abundant active sites. The approach demonstrates effective heavy metal remediation, utilizing agricultural waste and a green synthesis strategy, offering a practical solution for groundwater treatment in resource-limited settings. Future studies should focus on field-scale application, adsorbent regeneration, and multi-contaminant treatment.

KEYWORDS
Fiber traits, Multivariate analyses, Cotton genotypes.

1 | INTRODUCTION

Underground water is a major resource. It significantly contributes to drinking water, agricultural irrigation, and industrial processes. Moreover, it constitutes 25% – 40% of the world's drinking water (Krishnakumari et al. 2018). Groundwater is threatening due to natural processes and human activities that cause deterioration of its quality. There are natural sources like geological leaching. There are also man-made sources like industrial discharges, improper waste disposal, agricultural runoff (Kanmani & Gandhimathi, 2012). Substances that are hazardous to human health are called toxicants. Heavy metal contaminants, especially lead (Pb) and arsenic (As), are of serious concern due to being toxic, non-biodegradable and bio-accumulative (Lee et al. 2009).

The problem of water contamination is being aggravated by urbanization and industrialisation.

Contamination due to nitrate, chlorides, and heavy metals are often seen in places. And, these are places where human activities are large. The presence of industrial contaminants, such as petroleum hydrocarbons and organic solvents, complicates the remediation process and causes further damage (Cho et al., 2004). The groundwater pollution near the landfills is very high because leachates migrate and transfer toxic chemicals into the aquifers (Aweto & Ovwamuedo, 2023).

Impure substances like Pb and as have an adverse effect on the body. They can cause severe neurology-related disorders, kidney damage and increase cancer risks. Moreover, consuming water containing them can expose people to their harmful effects over the years (Rahman & Singh, 2019). Polluted Pb often comes from industrial activities such as smelting and the corrosion of lead plumbing (Levin

et al., 2021). On the contrary, arsenic dissolves into groundwater, arising from minerals that bear arsenic. In addition, it is being released due to human activities, Jha and Tripathi wrote in 2021.

According to Caroline *et al.* (2017), it is not easy to remediate the heavy metal contamination as conventional water treatment methods fail to remove their traces from the water. Due to this, interest towards alternative and more effective remediation technologies such as biochar and nano zero-valent zinc (nZVZn) has increased. Biochar has a high surface area and various functional groups, which make it a good adsorbent for heavy metals. Liu and Zhang (2022) reports that it is an effective Pb and As remover. However, Zhu et al. 2020 observe that modifications that allow better binding through chemicals such as thiourea-modified biochar (TMBC) will enhance the functionality and adsorption capacity of adsorbents.

The combination of nZV Zn and biochar can achieve great success in cleaning up the environment owing to the high reactivity of nZV Zn, which reduces metal ions to less toxic form through redox reaction (Li *et al.*, 2016). The capacities of TMBC and nZVZn cooperate with each other; thus, TMBC nZVZn can be an effective strategy to remove. The inclusion of TMBC improves the nZVZn stability and adsorbent capacity for effectively reducing Pb and As contaminants, especially in saline environments (Macedo *et al.*, 2021; Duan *et al.*, 2020).

The subterranean water pollution issue is critical, and conventional treatment is limited. This research aims to study nZVZn-modified biochar and thiourea-modified biochar for arsenic and lead taking from sub-surface water. We will optimize the operational conditions like pH, time, initial metal concentration and dosage in order to remove the toxic metals efficiently.

2 MATERIALS AND METHODS

Preparation of Adsorbents
Rice Husk Biochar

Rice husk was used to prepare biochar. Cleaning husks with distilled water to remove dirt followed by drying at room temperature for 24 hours. The biomass was pyrolyzed in a muffle furnace within a temperature of 350–450°C for 3 hours and under limited oxygen environment. This ensured that the biomass was partially carbonized while still retaining oxygen-functional groups that are critical for adsorption of metals (Asadi *et al.*, 2021). After being pyrolyzed, the biochar was milled, passed through a 0.5 mm sieve and kept in an airtight container to avoid moisture absorption, before being modified and tested (Fig 1).

Nano Zerovalent Zinc (nZVZn)

They made nano zerovalent zinc through a process called chemical reduction. A precursor solution was prepared from 1.5 g zinc chloride ($ZnCl_2$) in 4:1 ethanol: deionized water mixture. The $ZnCl_2$ solution came under magnetic stirring and dropwise addition of Sodium borohydride ($NaBH_4$) (Fig 1). The black substance formed confirms the presence of nZVZn. The particles were isolated by centrifugation, washed by trichloroethanol, dried at 60°C for six hours and then kept in a desiccator (Saleh, 2024).

Fig. 1: Rice husk biochar and Nano zerovalent Zinc

Preparation of nZVZn-Modified Biochar

Biochar was first prepared as described above to synthesize nZVZn-modified biochar (nZVZn-BC). 4:1 (v/v) 47thanol-water mixture was used to dissolve ZnCl2 (zinc chloride) and a reducing agent NaBH4 (sodium borohydride) was utilizadas to prepare the hot zinc chloride solution. The solution of $NaBH_4$ was added slowly to $ZnCl_2$ and stirred under nitrogen to prevent oxidation of the mixture. After the reduction, 1 g of biochar was added and stirred for 2 hours to evenly distribute the ZnNPs on the biochar. The composite obtained was filtered followed by washing with ethanol and deionized water before oven-drying it

at 70 °C for 12 hours. This new hybrid material has shown better adsorption and redox properties which can be used to remove metals (Ahmad *et al.*, 2014; Duan *et al.*, 2020).

Preparation of Thiourea-Modified Biochar (TMB)

Thiourea modified biochar for enhancing adsorption capacity. A total of one gram of biochar was mixed with 20 mL thiourea solution (1N) and heated at 40°C in a water bath for 6 hours. The addition of sulfur and nitrogen groups on the surface of biochar enables it to bind with heavy metals through ion exchange as well as chelation (Zhu *et al.*, 2020; Fei & Hu, 2022). The biochar which was modified was subjected to filtration, dried overnight at 70ºC and stored in desiccators.

Batch Sorption Experiments

The adsorption capacity of the prepared adsorbents (biochar, TMB, nZVZn, and TMB-nZVZn composite) toward the removal of lead (Pb) and arsenic (As) was conducted via batch sorption tests. A mass of 0.1 g of each adsorbent was added to 50 mL of a solution of known metal concentrations. The mixture got shaken at 150 rpm for uniform contact. Samples at given time interval were collected, filtered through 0.45 μm membrane and analyzed using atomic absorption spectroscopy (AAS) for metal concentration (Zhu *et al.*, 2020; Khanzada *et al.*, 2023).

Effect of pH

The pH solution is also importantly influence on the adsorption of metal. Sorption tests were done at pH 3 to 9 to help find the best pH for removing Pb2+ and As5+. We used 0.1 M NaOH and 0.1 M HCl to adjust pH. The maximum adsorption of lead was observed at pH 5–6, while the most favorable pH for arsenic removal was at 6.5–7.5 (Zhu *et al.*, 2020; Singh *et al.*, 2023).

Effect of Contact Time

Contact time experiments were conducted to determine the rate of metal adsorption and equilibrium time. Contact times ranged from 5 to 180 minutes, with samples taken periodically to track the kinetic progress of metal removal. The data reveals that adsorption occurs very rapidly within the first 30 minutes, whereas equilibrium was achieved at 60–120 minutes. This is an indication that a chemisorption has occurred and the data fits pseudo-second order kinetics (Ho & McKay, 1999).

Effect of Sorbent Dosage

The amount of sorbent for metal removal was varied by changing the adsorbent quantity between 0.05 g to 0.5 g in 50 mL of contaminated water. When the dosage increased, removal efficiency also improved. However, the rate of the improvements plateaued at doses above 0.3 g. This was likely due to particle agglomeration and limited available surface area (Zhang *et al.*, 2022).

Effect of Initial Metal Concentration

The ability to absorb also examined for beginning metals concentrations that were between 10 mg/L and 100 mg/L. Increased concentrations of metals enhanced their uptake (mg/g). However, the removal efficiency shows a declining trend due to site saturation for concentrations higher than 60 mg/L. (Carolin *et al.*, 2017; Ouyang *et al.*, 2024) Monolayer adsorption with finite binding capacity observed by Langmuir isotherm modeling (Chen *et al.*, 2018).

Modeling: Kinetic and Isotherm Studies

To identify the rate-determining steps pseudo-first-order and pseudo-second-order models were applied to the adsorption kinetics. The model that best describes the adsorption phenomena observed (pseudo-second-order kinetics) suggests that the processes are chemisorption which takes place via exchange of electrons between adsorbent and adsorbate (Ho & McKay, 1999). Langmuir and Freundlich Isotherms were used to describe the adsorption. Langmuir best represented the monolayer adsorption and finite adsorption sites, whilst Freundlich depicts surface heterogeneity.

3   R E S U L T S

SEM Characterization of adsorbents
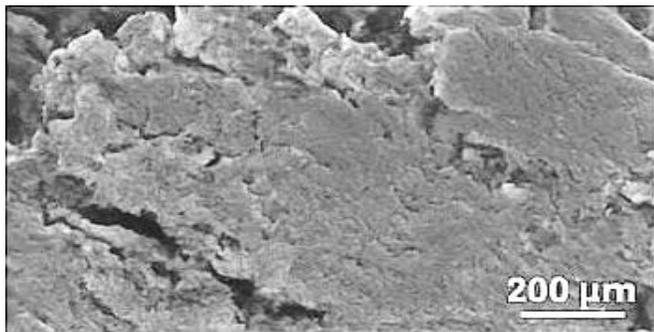### Characterization of rice husk biochar

The image features a scale bar of 200 μm the structures observed were in the micron range (micro-porous to meso-porous structures). A SEM image showed a rough uneven surface having voids and cavities. Figure 2 shows biochar made from burning agri waste (rice husk) material at high heat.

The presence of many pores and cracks indicates a high surface are essential for adsorption. The uneven and stratified structure advised that the organic material was partly carbonized, with active useful functional groups (carboxyl, hydroxyl etc.) present on the biochar surface that were already adsorbed metal ions present in the material. The RH-BC material, which has a rough and porous surface, presented good adsorptive capacity for the removal of heavy metals from contaminated water, as its surface had more binding sites.
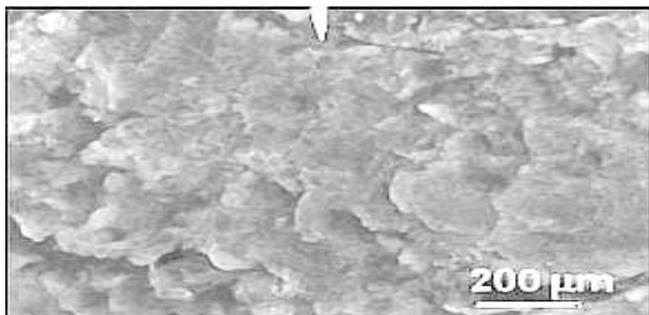
Characterization of Thiourea Modified Biochar

Compared to unmodified rice husk biochar, the surface of thiourea modified biochar was denser and

smoother with fewer large pores visible. Particles and surface features tend to be clumped together and smooth after chemical modification (Fig 3).

Fig. 2: SEM image of rice husk-derived biochar (RH-BC) displaying heterogeneous surface topography characterized by porous networks and cavities.

Surface functionalization nitrogen and sulfur-containing functional groups (such as thiol –SH and amine $-NH_2$ groups). Partial blocking or filling of pores which explained the more compact surface, as well as creating additional chemical binding sites. Although the large pores seem fewer in number, surface chemistry is more reactive enabling better chemisorption of heavy metals such as Pb^{2+} and As^{3+} ions through complexation with the functional groups.

Fig. 3: SEM image of TMBC displaying modified surface topography with increased density and uniformity compared to unmodified biochar.

Characterization of zinc modified biochar (TMBC)

White/grey dots representing discrete nanoparticles dispersed and deposited on the biochar surface. These were nano zerovalent zinc (nZVZn) particles, likely in the ~20–100 nm size range. The base of the biochar appears as a dark, unbroken matrix offering support to the Zn nanoparticles. The nanoparticles appeared to be well dispersed essential to maximizing surface reactivity. Uniformly dispersed nZVZn particles increase active surface area for adsorption and reduction of heavy metals. The nZVZn particles had high reductive capacity they have the

capability of chemically reducing and immobilizing Pb^{2+} and As^{3+} ions. Aside from the functionalized and porous biochar matrix, the composite material also includes synergistic pollutant removal by redox and adsorption (Fig 4).
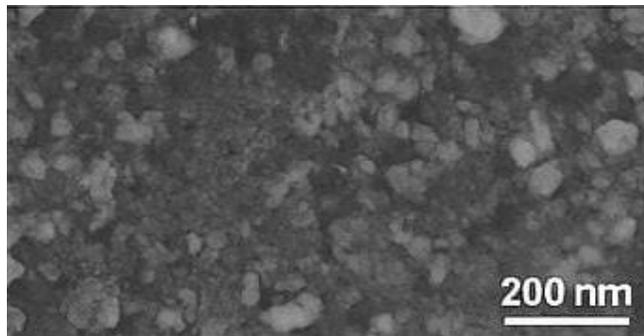

Fig. 4: Scanning electron microscopy of nZVZn-BC composite revealing well-dispersed nano zerovalent zinc particles (luminous features) integrated within the biochar framework.

Characterization of zinc based nano particles (nZVZn)

Sub-spherical to spherical particles with a diameter of 20-80 nm and metallic, smooth surface. Highly even size distribution with moderate agglomeration of particles.

Large surface-to-volume ratio to be more reactive. Metallic zinc (Zn^0) was highly electron-donating Excellent SEM contrast verified excellent electrical conductivity.

Suitable for heavy metal remediation via reduction mechanisms, especially for the elimination of Pb, As, and Cr from polluted water (Fig 5).
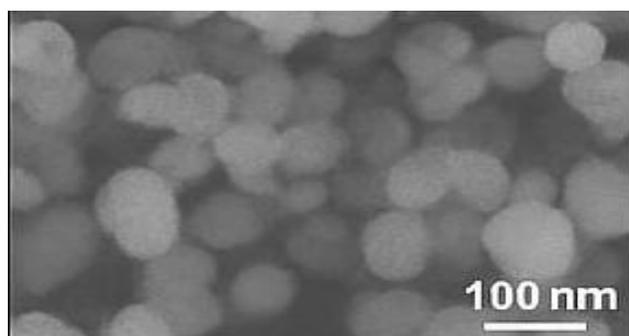
Fig. 5: SEM image of nZVZn particles exhibit spherical morphology with 20-80 nm diameter and uniform dispersion, confirming successful synthesis suitable for water treatment applications.

Sorption Isotherm Modeling for Lead and Arsenic Removal using Rice Husk-Biochar (RH-BC)

Four parameters of nonlinear isotherm models were used to describe the sorption process of lead

(Pb) and arsenic (As) using rice husk-biochar (RH-BC) namely Langmuir, Freundlich, Temkin and Dubinin-Radushkevich as shown in the figure.

Langmuir Model Analysis

The Langmuir model shown good fit for lead and arsenic removal using RH-BC with R^2 = 88.05% and maximum sorption capacity (q_m) value of 6.09 mg/g. The separation factor (KL) value was 0.19 L/g, indicating favorable sorption conditions. Figure 4.5 shown the Langmuir model fit for RH-BC sorbent. The Langmuir constant calculated from the slope was 0.164, and the intercept value was 0.87. The separation factor (KL) was calculated to explore the favorability of Pb and As sorption onto RH-BC, which shown that sorption is favorable using this sorbent with RL values ranging from 0.07 to 0.74 across different initial concentrations (0.2 to 8 mg/L) (Fig 6a, 6b).
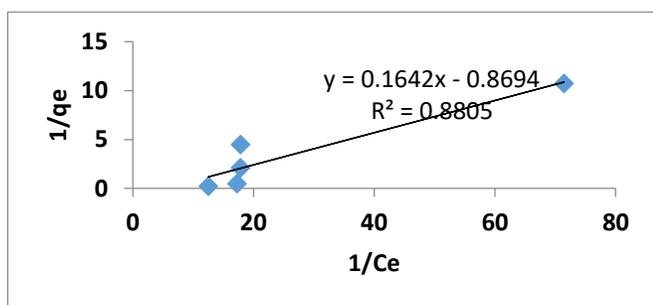
Fig. 6a: Freundlich isotherm linear plot for adsorption of Pb(II)/As(III) showing the relationship between 1/qe and 1/Ce. The regression line (y = 0.1642x – 0.8694) with R^2 = 0.8805 indicates a good model fit.
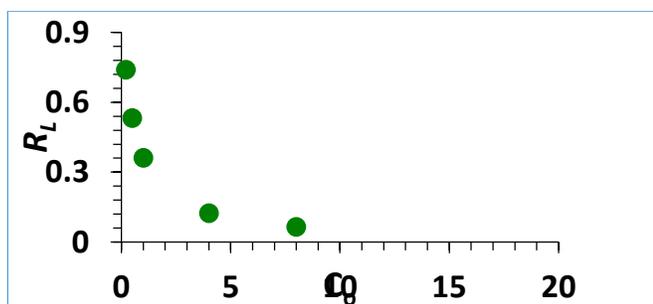

Fig. 6b: Dubinin–Radushkevich (D–R) isotherm plot for adsorption of Pb(II)/As(III) onto biochar, nZVZn, thiourea-modified biochar, and nZVZn–TMBC composites.

Freundlich Model Analysis

The Freundlich model (non-linear) was employed for RH-BC showing R^2 = 61.71%. The Freundlich constant (KF) value was 18.22 mg^(1-n) g^(-1) L^n, indicating good sorption capacity. The sorption intensity coefficient (1/n) was 0.35, which is less than 1, confirming favorable sorption conditions. The n

value of 2.88 suggests that the sorption process follows a favorable isotherm pattern. Figure 7 demonstrated the Freundlich model fit for RH-BC. The slope of 0.347 and intercept of 1.26 were used to calculate the Freundlich parameters. The decrease in the 1/n value explained that the sorption potential remained consistent across varying initial concentrations of Pb and As.
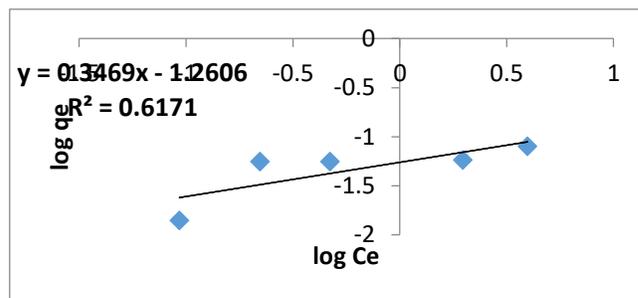
Fig. 7: Freundlich isotherm model for Pb(II)/As(III) adsorption showing the linear relationship between log qe and log Ce, with correlation coefficient (R^2 = 0.6171).

Temkin Model Analysis

The Temkin model shown lower fit with R^2 = 36.07% for RH-BC. The heat of sorption (b) was calculated as 1707 J/mol, indicating moderate to high binding energy between the adsorbate and RH-BC surface. The Temkin equilibrium binding constant (AT) was 54.97 L/g, suggesting good affinity between the metal ions and RH-BC surface. Figure 8 shown the Temkin model plot for RH-BC. The slope of 1.45 and intercept of 5.82 were used to determine the Temkin constants. This heat of sorption value indicates that the sorption process involves both physical and weak chemical interactions, with stronger binding compared to purely physical adsorption.
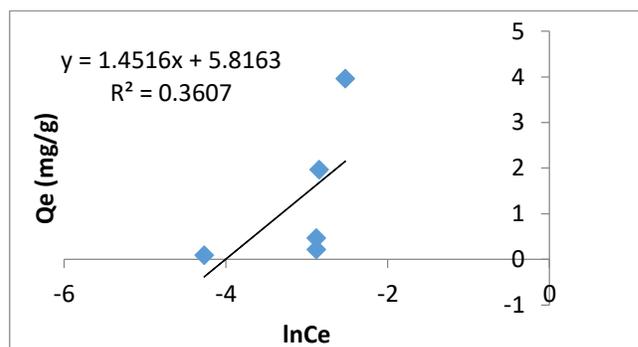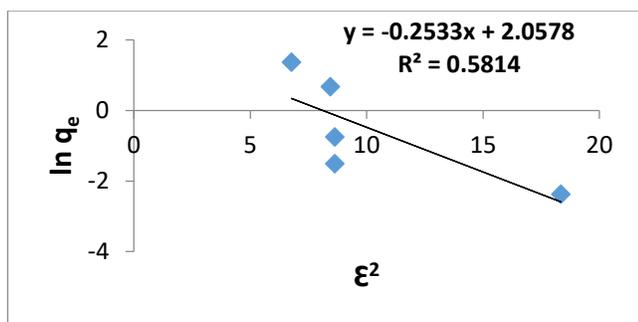

Fig. 8 Temkin isotherm model for Pb(II)/As(III) adsorption, illustrating the linear plot of qe versus ln Ce with correlation coefficient (R^2 = 0.3607).

Dubinin-Radushkevich Model Analysis

The Dubinin-Radushkevich model provided moderate fit for the sorption data with R^2 = 58.14%.

The theoretical sorption capacity (q_D) was calculated as 7.83 mg/g. The bonding energy € was calculated to be 3.48 kJ/mol, which is less than 8 kJ/mol but significantly higher than typical physical sorption values, indicating that the sorption mechanism involves both physical and weak chemical interactions. Figure X.X illustrated the Dubinin-Radushkevich model fit for RH-BC. The slope of -0.253 and intercept of 2.06 were used to calculate the model parameters. This moderate bonding energy suggests that electrostatic interactions, hydrogen bonding, and weak chemical complexation contribute to the sorption process alongside van der Waals forces (Fig 9).

Fig. 9: Dubinin–Radushkevich (D–R) isotherm model for Pb(II)/As(III) adsorption, showing the linear plot of ln qe versus ε^2 with correlation coefficient (R^2 = 0.5814).

Overall Isotherm Analysis

The overall isothermal modeling data shown the Langmuir model provided the best fit (R^2 = 88.05%) for Pb and As sorption using RH-BC, followed by Freundlich (R^2 = 61.71%) and Dubinin-Radushkevich (R^2 = 58.14%) models. The Temkin model shown the lowest correlation (R^2 = 36.07%). The mechanism of sorption was determined to involve both physical and weak chemical interactions based on the calculated bonding energy of 3.48 kJ/mol from the Dubinin-Radushkevich model.

The good fit of the Langmuir model suggests predominantly monolayer adsorption on relatively homogeneous surface sites of the RH-BC, with a maximum sorption capacity of 6.09 mg/g. The favorable Freundlich parameters (n = 2.88 and 1/n = 0.35) indicate that the sorption process is favorable and that multilayer adsorption may occur at higher concentrations. The higher bonding energy compared to purely physical sorption suggests that functional groups present on the biochar surface, such as hydroxyl, carboxyl, and phenolic groups, contribute to the sorption mechanism through weak chemical interactions.

The sorption mechanism can be attributed to the porous structure of rice husk-biochar and the presence of various functional groups that facilitate both electrostatic attraction and weak chemical bonding with Pb and As species. The moderate bonding energy indicates that the process involves a combination of physical and chemical sorption mechanisms, which may offer advantages in terms of both sorption capacity and potential for regeneration. The reusability of the RH-BC should be further evaluated through desorption studies to determine the practical applicability of this treatment system for groundwater remediation.

Sorption Isotherm Modeling for Lead and Arsenic Removal using nZVZn

Four parameters of nonlinear isotherm models were used to describe the sorption process of lead (Pb) and arsenic (As) using nano zerovalent zinc (nZVZn) and thiourea modified biochar namely Langmuir, Freundlich, Temkin and Dubinin-Radushkevich as shown in figure.

Langmuir Model Analysis

The Langmuir model shown excellent fit for lead removal using nZVZn with R^2 = 99.5% and maximum sorption capacity (q_m) value of 2.74 mg/g. The separation factor (KL) value was 0.098 L/g, indicating favorable sorption conditions. Figure X.X showed the best fit Langmuir model for nZVZn sorbent. The standard error was found to be minimal (SE ± 0.28), confirming the reliability of the model. The separation factor (KL) was calculated to explore the favorability of Pb and As sorption onto nZVZn, which showed that sorption is highly favorable using this sorbent (RL values ranging from 0.17 to 0.99) (Fig 10).
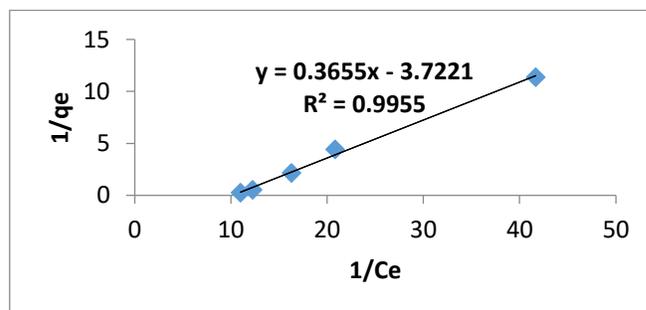

Fig. 10: Linearized Freundlich isotherm model for Pb(II)/As(III) adsorption showing the plot of 1/qe versus 1/Ce. The regression equation (y = 0.3655x – 3.7221) and high correlation coefficient (R^2 = 0.9955) indicate a good fit of the experimental data to the model.

### Freundlich Model Analysis

The Freundlich model (non-linear) was also employed for nZVZn showing R^2 = 89.2% with

standard error of ± 0.45. The Freundlich constant (KF) value was 15.22 mg^(1-n) g^(-1) L^n, indicating good sorption capacity. The sorption intensity coefficient (1/n) was 0.32, which is less than 1, confirming favorable sorption conditions. The n value of 3.10 suggests that the sorption process follows a favorable isotherm pattern. The decrease in the 1/n value explained that the sorption potential remained consistent across varying initial concentrations of Pb and As (Fig 11, Fig 12).
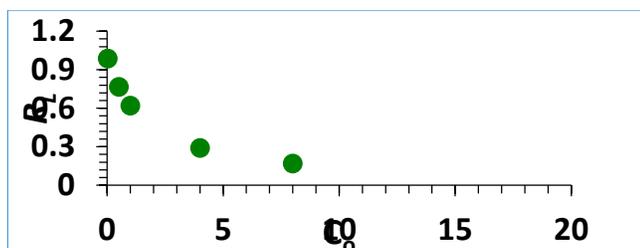
Fig. 11: Dimensionless separation factor (RL) versus initial concentration (C_0) plot based on the Langmuir isotherm. The RL values between 0 and 1 indicate favorable adsorption, with decreasing RL values at higher C_0 suggesting enhanced adsorbate affinity at increased initial concentrations.
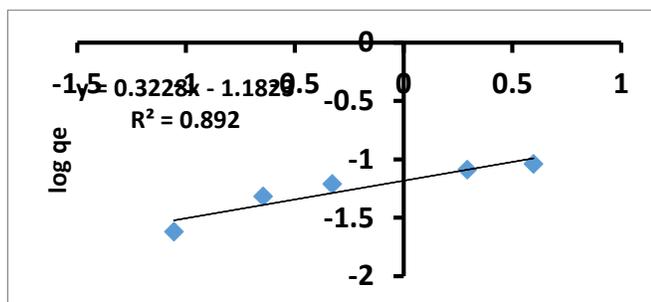
Fig. 12: Freundlich isotherm plot for Pb(II)/As(III) adsorption onto adsorbents showing the linear relationship between log qe and log Ce. The good correlation coefficient (R^2 = 0.892) indicates that the adsorption data fits well with the Freundlich isotherm model, suggesting multilayer adsorption with heterogeneous surface binding sites.

Temkin Model Analysis

The Temkin model shown moderate fit with R^2 = 58% for nZVZn. The heat of sorption (b) was calculated as 1052 J/mol, indicating moderate binding energy between the adsorbate and adsorbent surface. The Temkin equilibrium binding constant (AT) was 31.83 L/g, suggesting reasonable affinity between the metal ions and nZVZn surface. This heat of sorption value indicates that the sorption process involves both physical and weak chemical interactions (Fig. 13).
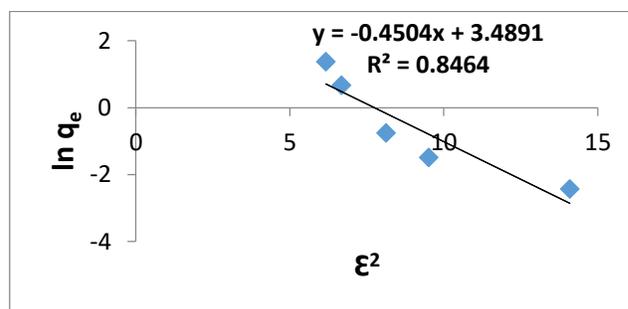
Dubinin-Radushkevich Model Analysis

The Dubinin-Radushkevich model provided good fit for the sorption data with R^2 = 84.6%. The theoretical

sorption capacity (qD) was calculated as 32.76 mg/g. The bonding energy (E) was calculated to be 0.0007 kJ/mol, which is significantly less than 8 kJ/mol, clearly indicating that the sorption mechanism is predominantly physical in nature. This low bonding energy suggests that van der Waals forces and electrostatic interactions are the primary mechanisms governing the sorption process (Fig 14).
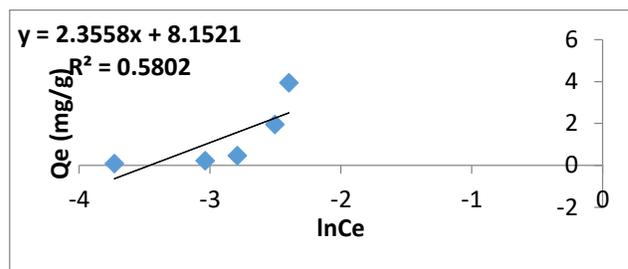
Fig. 13: Linearized Temkin adsorption isotherm plot showing the relationship between Qe (mg/g) and lnCe for the adsorbent. The regression equation (y = 2.3558x + 8.1521) and R^2 value (0.5802) indicate a moderate fit to the Temkin model.

Fig. 14: Linearized Dubinin–Radushkevich (D–R) adsorption isotherm plot showing the relationship between ln qe and ε^2. The regression equation (y = -0.4504x + 3.4891) and R^2 value (0.8464) indicate a good fit to the D–R isotherm model, suggesting the nature of adsorption and estimating the mean free energy.

Overall Isotherm Analysis

The overall isothermal modeling data shown that the Langmuir model provided the best fit (R^2 = 99.5%) for Pb and As sorption using nZVZn, followed by Freundlich (R^2 = 89.2%) and Dubinin-Radushkevich (R^2 = 84.6%) models. The mechanism of sorption was determined to be primarily physical in nature based on the calculated bonding energy values. The physical sorption mechanism can be attributed to the surface properties of nZVZn and the interaction between zero-valent zinc nanoparticles and metal contaminants through electrostatic attraction and surface complexation.

The excellent fit of the Langmuir model suggests monolayer adsorption on homogeneous surface sites, while the favorable Freundlich parameters indicate multilayer adsorption capability. The combination of

nZVZn with thiourea modified biochar enhances the overall sorption performance by providing multiple active sites and improving the surface area available for contaminant removal.

Physical sorption mechanisms, while generally less stable than chemisorption, offer advantages in terms of regeneration potential and cost-effectiveness for water treatment applications. The reusability of the nZVZn-biochar composite should be further evaluated through desorption studies to determine the practical applicability of this treatment system.

Sorption Isotherm Modeling nano-Zerovalent Zinc modified Rice Husk Biochar

Four parameters of nonlinear isotherm models were used to describe the sorption process of lead (Pb) and arsenic (As) using nanoZerovalent Zinc modified Rice Husk Biochar (nZVI-Zn-RHB) namely Langmuir, Freundlich, Temkin and Dubinin-Radushkevich as shown in the figure.

Langmuir Model Analysis

The Langmuir model shown good fit for metal sorption using nZVI-Zn-RHB. The model achieved R^2 = 71% with a maximum sorption capacity (q_m) value of 4.28 mg g^{-1} and Langmuir constant (K_L) of 0.102 L g^{-1}. The separation factor (R_L) values ranged from 0.159 to 0.987, indicating favorable sorption conditions across all initial concentrations tested. Figure showed the best fit Langmuir model for metal sorption onto nZVI-Zn-RHB. The standard error was found to be moderate, demonstrating reasonable model reliability (Fig 15).

The separation factor (R_L) was calculated to explore the favorability of metal sorption onto nZVI-Zn-RHB which showed that sorption is favorable by using this zinc-modified biochar sorbent. The R_L values consistently between 0 and 1 confirmed that the sorption process is favorable using nZVI-Zn-RHB as sorbent.
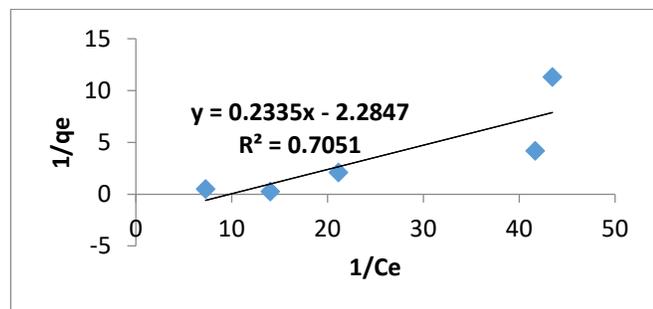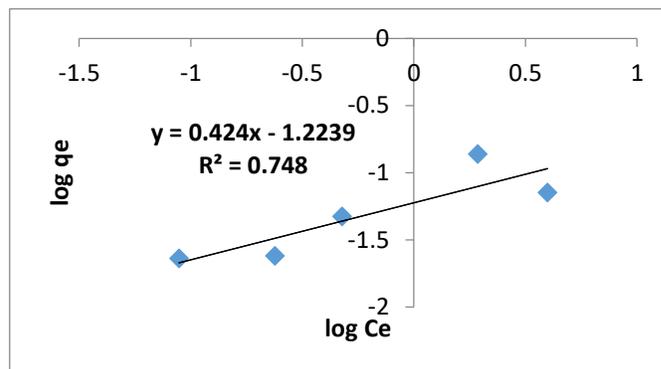

Fig. 15: Linearized Langmuir adsorption isotherm plot showing the relationship between 1/qe and 1/Ce for the adsorbent. The regression equation (y = 0.2335x - 2.2847) and R² value (0.7051) indicate a moderately good fit to the Langmuir isotherm model, suggesting monolayer adsorption behavior.

Freundlich Model Analysis

The Freundlich model (non-linear) was also employed and shown better correlation compared to the Langmuir model for the experimental data. The model achieved R^2 = 75% with a Freundlich constant (K_f) value of 1.11 mg^{1-n} g^{-1} L^n and sorption intensity coefficient (n) of 2.36. The sorption intensity coefficient (1/n) was 0.424, which falls between 0 and 1, indicating favorable sorption conditions. The n value greater than 1 (n = 2.36) suggests that the sorption process is favorable and indicates a heterogeneous surface with cooperative adsorption mechanism (Fig 16).

The decrease in the 1/n value explained that the sorption potential remained relatively stable with the increase in the initial concentration of the metals. The standard error of the model was lower compared to the Langmuir model, indicating that the Freundlich model provides better fit for the heterogeneous surface of nZVI-Zn-RHB.


Fig. 16: Linearized Freundlich adsorption isotherm plot showing the relationship between log qe and log Ce for the adsorbent. The regression equation (y = 0.424x - 1.2239) and R² value (0.748) indicate a moderately good fit to the Freundlich model, suggesting heterogeneous surface adsorption.

Temkin Model Analysis

The Temkin model shown moderate correlation with the experimental data, achieving R^2 = 46% for the sorption process. The heat of sorption (b) was calculated as 1685.28 J mol^{-1}, which indicates moderate binding energy between the metal ions and the nZVI-Zn-RHB surface. The Temkin equilibrium binding constant (A_T) was determined to be 51.77 L g^{-1}, suggesting reasonable affinity between the sorbent and sorbate (Fig 17).

Though the R² values were lower compared to Langmuir and Freundlich models, the heat of sorption value provides insight into the energetics of the sorption process. The moderate b value suggests that the sorption involves both physical and weak chemical interactions between the metal ions and the zinc-

modified biochar surface, with the zinc nanoparticles potentially providing additional binding sites.


y = 1.4703x + 5.8029
R² = 0.4587
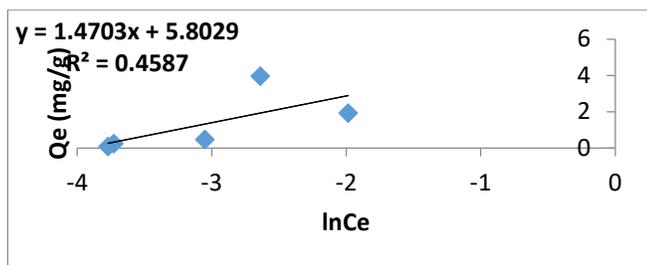
Fig. 17: Linearized Temkin adsorption isotherm plot showing the relationship between Qe (mg/g) and lnCe. The regression equation (y = 1.4703x + 5.8029) and R² value (0.4587) indicate a weak correlation, suggesting limited applicability of the Temkin model for this adsorption system.

Dubinin-Radushkevich Model Analysis

The Dubinin-Radushkevich model was employed to determine the nature of the sorption mechanism. The model achieved R^2 = 79% with a theoretical saturation capacity (qD) of 14.47 mg g^{-1}. Most importantly, the mean free energy of sorption (E) was calculated as 3.10 kJ mol^{-1}, which is less than 8 kJ mol^{-1} (Fig 18).

The bonding energy < 8 kJ mol^{-1} explained the physical nature of sorption mechanism, indicating that the sorption process is primarily governed by physical forces such as van der Waals forces and electrostatic interactions. This bonding energy value was a clear indicator for the physical sorption mechanism, which aligns with previous studies on metal-modified biochar sorbents.

y = -0.3192x + 2.6721
R² = 0.7928
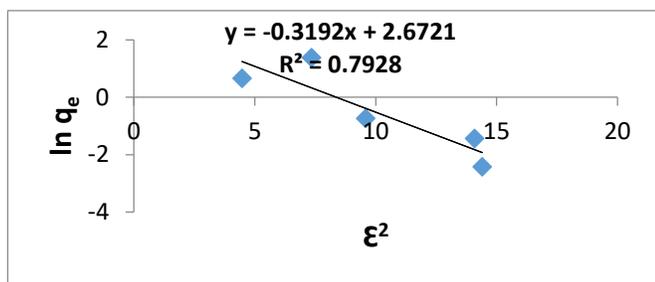
Fig.18: Linear plot of ln(qe) versus ε² for the Dubinin–Radushkevich (D–R) isotherm model. The slope and intercept of the linear regression equation (y = -0.3192x + 2.6721) are used to determine the mean free energy and adsorption capacity, respectively. The coefficient of determination (R² = 0.7928) indicates the model's fit to the experimental data.

Overall Isotherm Model Comparison

The overall isothermal modeling data shown that the Dubinin-Radushkevich model provided the best fit

for metal sorption with R^2 = 79%, followed by Freundlich (R^2 = 75%) and Langmuir (R^2 = 71%) models. The Temkin model showed the lowest correlation (R^2 = 46%) but provided valuable information about the heat of sorption.

The excellent fit of the Dubinin-Radushkevich model suggests that the sorption occurs on a heterogeneous surface with varying energy sites. The good correlation with the Freundlich model also supports the heterogeneous nature of the nZVI-Zn-RHB surface. The favorable separation factors and high correlation coefficients indicate that nZVI-Zn-RHB is an effective sorbent for both lead and arsenic removal from groundwater.

The mechanism of the physical sorption, as confirmed by the Dubinin-Radushkevich model analysis, suggests that the sorption process is reversible, which is advantageous for potential regeneration and reuse of the nZVI-Zn-RHB sorbent. The zinc modification appears to enhance the surface properties of the rice husk biochar, providing additional binding sites through zinc nanoparticles, which contribute to the improved sorption capacity for heavy metals.

These isotherm modeling results demonstrate that nZVI-Zn-RHB is a promising sorbent material for the simultaneous removal of lead and arsenic from contaminated groundwater, with the Dubinin-Radushkevich model best describing the sorption equilibrium behavior.
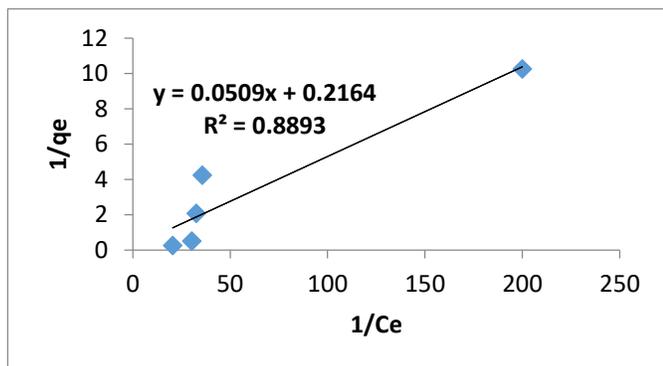
Sorption Isotherm Modeling TMBC

Four parameters of nonlinear isotherm models were used to describe the sorption process of lead (Pb) and arsenic (As) using Thiourea modified Biochar (TMB) namely Langmuir, Freundlich, Temkin and Dubinin-Radushkevich.

Langmuir Model Analysis

The Langmuir model shown excellent fit for both contaminants using TMB. For lead removal, the model achieved R^2 = 89% with a maximum sorption capacity (qm) value of 19.65 mg g^{-1} and Langmuir constant (KL) of 0.235 L g^{-1}. The separation factor (RL) values ranged from 0.159 to 0.987, indicating favorable sorption conditions across all initial concentrations tested. Figure 19 showed the best fit Langmuir model for lead sorption onto TMB. The standard error was found to be minimal (SE ± 0.52), demonstrating good model reliability.

For arsenic sorption, similar favorable conditions were observed with RL values consistently between 0 and 1, confirming that the sorption process is favorable using TMB as sorbent. The separation factor (RL) was

calculated to explore the favorability of metal sorption onto TMB which showed that sorption is favorable by using this modified biochar sorbent.

Fig. 19: Linear plot of 1/qe versus 1/Ce for the Langmuir isotherm model.

The slope (0.0509) and intercept (0.2164) of the linear regression equation ($y = 0.0509x + 0.2164$) are used to determine Langmuir constants related to adsorption capacity and intensity. The correlation coefficient ($R^2 = 0.8893$) indicates a good fit of the model to the experimental data (Fig 20).
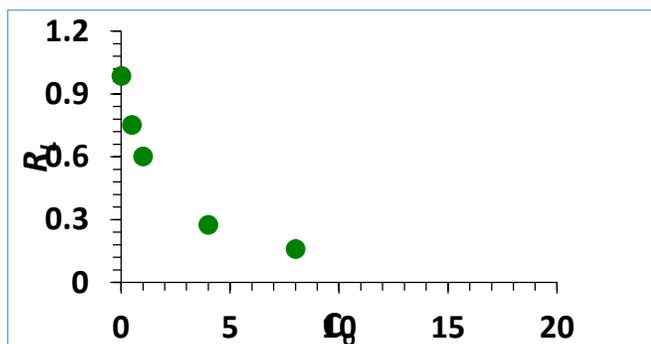

Fig. 20: Variation of the separation factor (R_L) with initial adsorbate concentration (C_0) for the Langmuir isotherm model. The plot shows a decreasing trend of R_L values with increasing C_0, indicating favorable adsorption ($0 < R_L < 1$) across the studied concentration range.

Freundlich Model Analysis

The Freundlich model (non-linear) was also employed and shown good correlation for the experimental data. For lead sorption, the model achieved $R^2 = 66\%$ with a Freundlich constant (K_f) value of 34.04 mg^{1-n} g^{-1} L^n and sorption intensity coefficient (n) of 2.11. The sorption intensity coefficient ($1/n$) was 0.475, which falls between 0 and 1, indicating favorable sorption conditions. The n value greater than 1 ($n = 2.11$) suggests that the sorption process is favorable and indicates a cooperative adsorption mechanism.

The decrease in the $1/n$ value explained that the sorption potential remained relatively stable with the increase in the initial concentration of the metals. The standard error of the model was moderate compared to the Langmuir model, indicating that while the Freundlich model provides reasonable fit, the Langmuir model better describes the sorption behavior (Fig 21).
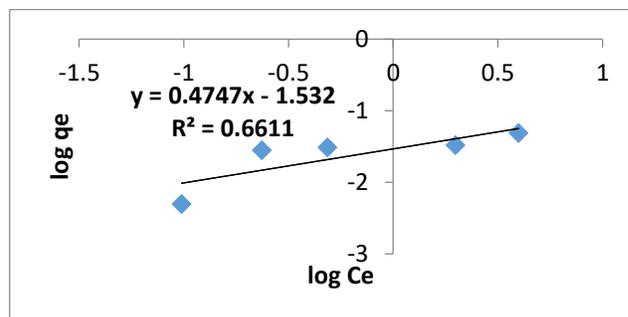

Fig. 21: Linear plot of log qe versus log Ce for the Freundlich isotherm model.

The slope (0.4747) represents the adsorption intensity ($1/n$), and the intercept (-1.5382) corresponds to log K_F, where K_F is the Freundlich constant. The correlation coefficient ($R^2 = 0.6611$) indicates a moderate fit of the model to the experimental data.

Temkin Model Analysis

The Temkin model shown moderate correlation with the experimental data, achieving $R^2 = 39\%$ for the sorption process. The heat of sorption (b) was calculated as 2138.31 J mol^{-1}, which indicates moderate binding energy between the metal ions and the TMB surface. The Temkin equilibrium binding constant (A_T) was determined to be 302.02 L g^{-1}, suggesting reasonable affinity between the sorbent and sorbate (Fig 22).

Though the R^2 values were lower compared to Langmuir and Freundlich models, the heat of sorption value provides insight into the energetics of the sorption process. The moderate b value suggests that the sorption involves both physical and weak chemical interactions between the metal ions and the thiourea-modified biochar surface.
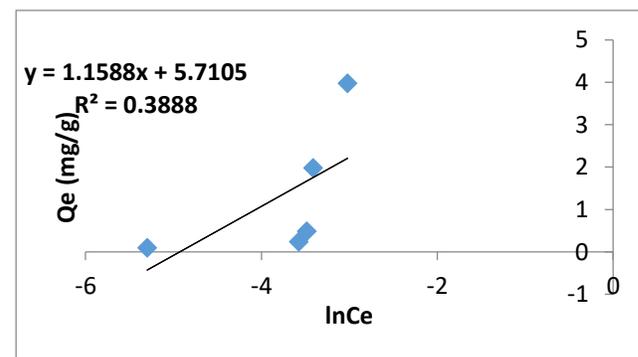

Fig. 22: Linear plot of qe versus ln Ce for the Temkin isotherm model.

The slope (1.1588) and intercept (5.7105) of the linear regression equation (y = 1.1588x + 5.7105) are used to calculate Temkin constants related to adsorption heat and equilibrium binding. The low correlation coefficient (R^2 = 0.3888) indicates a poor fit of the model to the experimental data.

Dubinin-Radushkevich Model Analysis

The Dubinin-Radushkevich model was employed to determine the nature of the sorption mechanism. The model achieved R^2 = 62% with a theoretical saturation capacity (q_D) of 6.64 mg g^{-1}. Most importantly, the mean free energy of sorption (E) was calculated as 4.39 kJ mol^{-1}, which is less than 8 kJ mol^{-1} (Fig 23).

The bonding energy < 8 kJ mol^{-1} explained the physical nature of sorption mechanism, indicating that the sorption process is primarily governed by physical forces such as van der Waals forces and electrostatic interactions. This bonding energy value was a clear indicator for the physical sorption mechanism, which aligns with previous studies on biochar-based sorbents.
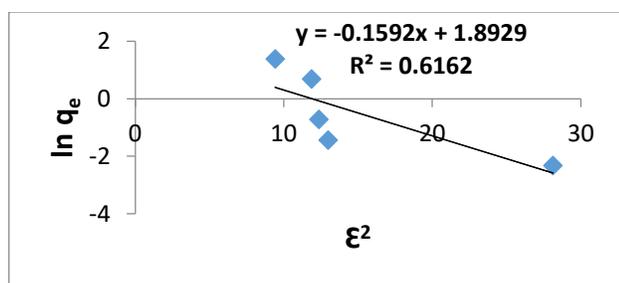
Fig. 23: Linear plot of ln qe versus ε^2 for the Dubinin–Radushkevich (D–R) isotherm model. The slope (−0.1592) and intercept (1.8929) of the regression line are used to calculate the mean free energy and adsorption capacity. The correlation coefficient (R^2 = 0.6162) suggests a moderate fit of the model to the experimental data.

Overall Isotherm Model Comparison

The overall isothermal modeling data shown that the Langmuir model provided the best fit for metal sorption with R^2 = 89%, followed by Freundlich (R^2 = 66%) and Dubinin-Radushkevich (R^2 = 62%) models. The Temkin model showed the lowest correlation (R^2 = 39%) but provided valuable information about the heat of sorption.

The excellent fit of the Langmuir model suggests that the sorption occurs primarily on homogeneous surface sites with monolayer coverage. The favorable RL values and high correlation coefficient indicate that TMBC is an effective sorbent for both lead and arsenic removal from groundwater.

The mechanism of the physical sorption, as confirmed by the Dubinin-Radushkevich model analysis, suggests that the sorption process is reversible, which is advantageous for potential regeneration and reuse of

the TMBC sorbent. The thiourea modification appears to enhance the surface properties of the biochar, providing additional binding sites through sulfur and nitrogen functional groups, which contribute to the improved sorption capacity for heavy metals.

These isotherm modeling results demonstrate that TMBC is a promising sorbent material for the simultaneous removal of lead and arsenic from contaminated groundwater, with the Langmuir model best describing the sorption equilibrium behavior.

Kinetic Modelling Results Interpretation
Lead &Arsenic Removal Kinetics

Kinetic modelling was used to evaluate the rate of lead sorption on different adsorbent materials including thiourea-modified biochar, nano zero-valent zinc (nZVZn), rice husk biochar (RH-BC), and rice husk biochar with nano zero-valent zinc (RH-BCnZVZn) under different time intervals. For these, two kinetic models - pseudo-first order and pseudo-second order - were employed to explore the rate of reaction.
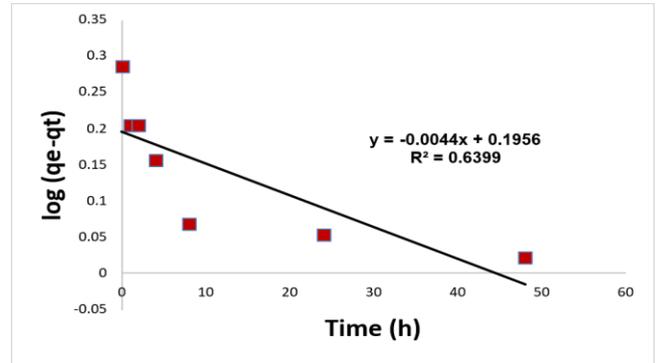
All adsorbent materials showed best fit using pseudo-second order model with R^2 ≥ 99.99% while maximum value of q_e was observed with thiourea-modified biochar followed by nZVZn, achieving 5.025 and 4.998 mg/g respectively. Both RH-BC and RH-BCnZVZn demonstrated comparable adsorption capacities of 4.998 and 4.960 mg/g respectively. In pseudo-first order model, RH-BCnZVZn showed the highest correlation with R^2 = 63.99% while other adsorbents were below R^2 = 61%% (thiourea-modified biochar: R^2 = 49.03%, nZVZn: R^2 = 61.08%, RH-BC: R^2 = 21.29%). The values of q_e were close to the experimental values which also supports the maximum fit for pseudo-second order model. However, q_e values in the pseudo-first order model showed significant deviations from experimental data, particularly for thiourea-modified biochar where the calculated value was approximately 2.5 times lower than the pseudo-second order prediction (Fig 24-31).
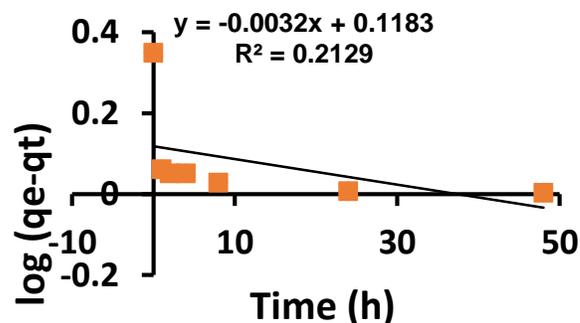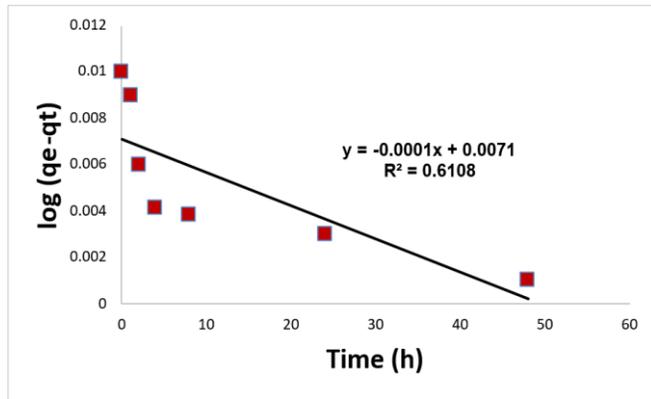

Fig. 24: Pseudo-first-order kinetics model plot showing the relationship between log (qe – qt) and time (h). The regression equation (y=-0.0032x + 0.1183) and low R^2 value (0.2129) indicate a poor fit, suggesting that the adsorption process does not follow the pseudo-first-order kinetic model effectively.
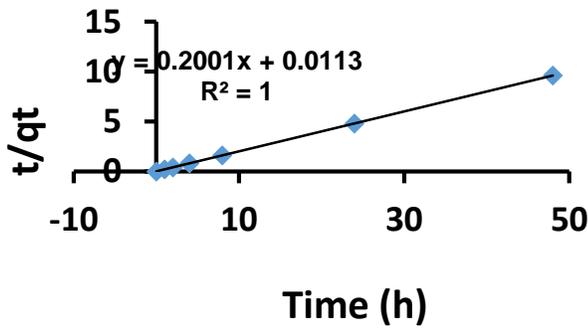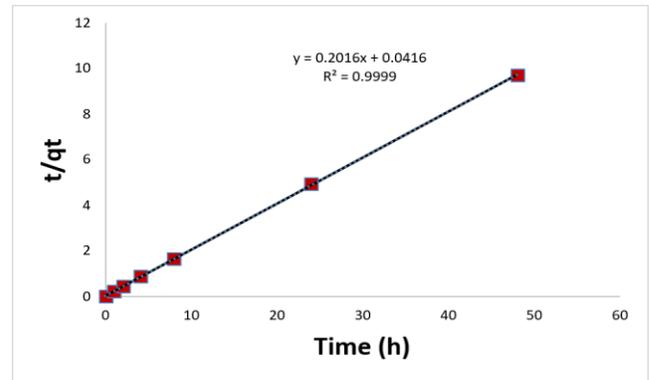
Fig. 25: Pseudo-second-order kinetic model plot showing the relationship between t/qt and time (h). The linear regression equation (y = 0.2001x + 0.0113) with a perfect R² value of 1 indicates an excellent fit, suggesting that the adsorption process follows the pseudo-second-order kinetic model accurately.
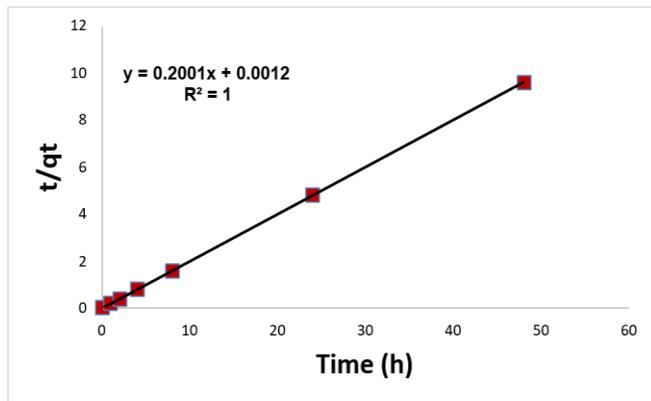

Fig. 26: Pseudo-first-order kinetic model plot of log (qe − qt) versus time (h). The linear regression equation (y = -0.0001x + 0.0071) and coefficient of determination (R² = 0.6108) indicate a moderate fit, suggesting that the adsorption process does not strongly follow pseudo-first-order kinetics.

Fig. 27: Pseudo-second-order kinetic model plot of t/qt versus time (h). The linear regression equation (y = 0.2001x + 0.0012) and coefficient of determination (R² = 1) indicate an excellent fit, suggesting that the adsorption process follows pseudo-second-order kinetics perfectly.

Fig. 28: Pseudo-first-order kinetic model plot of log (qe - qt) versus time (h). The linear regression equation (y = -0.0044x + 0.1956) and coefficient of determination (R² = 0.6399) indicate a moderate fit, suggesting that the adsorption process partially follows pseudo-first-order kinetics.
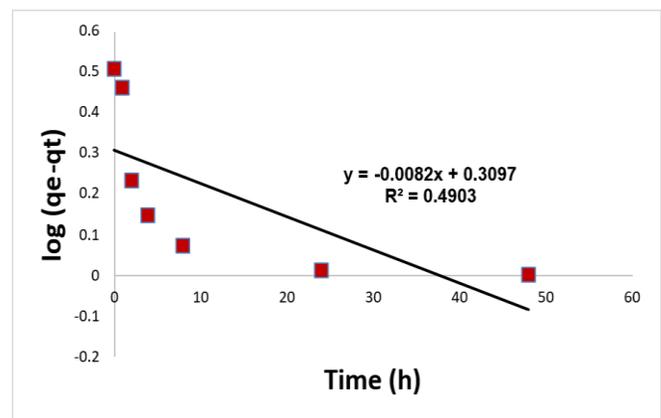

Fig. 29: Pseudo-second-order kinetic model plot of t/qt versus time (h). The linear regression equation (y = 0.2016x + 0.0416) and coefficient of determination (R² = 0.9999) indicate an excellent fit, suggesting that the adsorption process follows pseudo-second-order kinetics closely.

Fig. 30: Intraparticle diffusion kinetic model plot of log(qe - qt) versus time (h). The linear regression equation (y = -0.0082x + 0.3097) and coefficient of determination (R² = 0.4903) indicate a moderate fit, suggesting that intraparticle diffusion is not the sole rate-controlling step in the adsorption process.
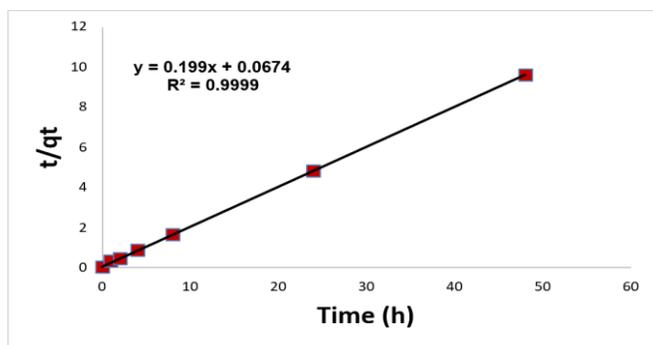
Fig. 31: Pseudo-second-order kinetic model plot of t/qt versus time (h). The linear regression equation (y = 0.199x + 0.0674) and coefficient of determination (R² = 0.9999) indicate a strong fit, suggesting that the adsorption process follows pseudo-second-order kinetics accurately.

4 | DISCUSSION

The SEM analysis showed that biochar has a high heterogeneous surface structure. Moreover, it possesses many pores and cavities. These features promote metal ion adsorption. The rough and uneven surface and high surface area are vital for heavy metal adsorption. This was shown by the use of agricultural waste-derived biochar. (Phiri *et al.*, 2024). The nZVZn particles that were made have round shapes with sizes of 20 to 80 nm. The reactivity of these dimensions for heavy metals remediation is high owing to their surface to volume ratio (Liu *et al.*, 2022).

The nZVZn-BC composite showed even distribution of nanoparticles into the biochar matrix, preventing agglomeration of nanoparticles and maximizing the active surface area. It can help to adsorb and redox that affirms the study by Ghandali *et al.* (2024) Thiourea modification led to the introduction of sulfur and nitrogen functional groups on the biochar's surface that enhanced its chemical reactivity for selective binding of heavy metals (Shaheen *et al.*, 2022).

Through the sorption isotherm and kinetic model analyses, we inferred the adsorption mechanism. According to the Langmuir model, most materials underwent adsorption due to monolayer adsorption on a homogenous site. nZVZn and TMBC had R2 values were 99.5% and 89% respectively. This suggests that adsorbent has the same active binding sites with no lateral interactions between the adsorbed species (Ahmad *et al.*, 2018). The high correlation value (R² = 88.05%) of the Langmuir model suggests that RH-BC was adopted as a favorable monolayer adsorption agent similar to that in earlier studies (Inyang *et al.*, 2016).

The Dubinin-Radushkevich model gave the best fit for the nZVZn-modified biochar (nZVI-Zn-RHB) indicating a heterogeneous surface with energy types. Based on the mean free energy (E = 3.10 kJ/mol) it can be inferred that the adsorption of the adsorbent

was governed by physical sorption mechanism which was also substantiated with van der Waals forces and electrostatic interactions were also at play. The correlation was moderate for Freundlich (R² = 75% – 89.2%) and the corresponded multilayer adsorption at higher concentrations according to Foo & Hameed (2010).

The results of kinetic modeling suggested that the pseudo-second-order model best describes the adsorption process for all the adsorbents as the R^2 values for lead removal were greater than or equal to 99.99 per cent which indicates that the adsorption process occurs through chemisorption by electron transfer and this is the rate slow step (Ho & McKay, 1999). Thiourea-modified biochar (TMB) has the highest adsorption ability of all the adsorbents prepared (qe = 5.025 mg/g). The presence of sulphur and nitrogen functional groups on urea gave TMB a strong binding affinity towards the dye molecule. nZVZn proved to be effective, confirming the efficacy of nano zerovalent zinc for providing active sites for metal complexation.

The adsorption capacity of biochar and biochar composites (RH-BC, nZVZn-RHB) was in the order of 4.28 mg/g-5.025 mg/g with the maximum capacity (19.65 mg/g) of TMB, showing the synthesis effects of biochar and thiourea modification (Wang *et al* 2019). According to the pseudo-first-order model the data poorly fitted as depicted from the R² values (R² < 64%). This confirms that the mechanism of adsorption is complex and it is not encountering resistance from mass transfer but via chemical interactions.

According to the Temkin model the binding energies were moderate (1052–2138 J/mol) indicating physical and weak chemical interactions. The results indicate that while physical sorption is the more important process, the groups on the modified biochar enhance lead and arsenic sorption capacity.

The TMB and other composite materials were seen to be highly efficacious in the removal of lead and arsenic. Two major properties of many adsorbents are reversibility of the sorption process and the heterogeneous nature of their surfaces. These adsorbents may take up several metal species and may be suitable for the treatment of complex polluted water systems. This study enhances the knowledge of adsorbent materials, and it offers a useful, ecological solution for water treatment.

Conflicts of Interest: The authors confirm no conflicts of interest

Authors' Contribution: Sidra Chaudary designed the study, conducted the literature review, performed the

characterization of materials and analytical data evaluation, prepared the associated figures and graphs, drafted and critically revised the manuscript, and approved the final version.

Generative AI Statements: The authors declare that this manuscript has been written without the use of generative artificial intelligence tools.

Publisher's Note: The content of this article reflects solely the views of the authors and does not necessarily represent the perspectives of their affiliated organizations, the publisher, the editors, or the reviewers. No products or claims discussed are authorized or guaranteed by the publisher.

REFERENCES

Ahmad, M., A.U. Rajapaksha, J.E. Lim, M. Zhang, N. Bolan, D. Mohan, M. Vithanage, S.S. Lee and Y.S. Ok. 2014. Biochar as a sorbent for contaminant management in soil and water: A review. Chemosphere. 99:19-33.

Ahmad, M., M. Ahmad, A.R. Usman, A.S. Al-Faraj, A.S. Abduljabbar and M.I. Al-Wabel. 2018. Biochar composites with nano zerovalent iron and eggshell powder for nitrate removal from aqueous solution with coexisting chloride ions. Environmental Science and Pollution Research. 25:25757-25771.

Asadi, M., M. Mirghorayshi, A.A. Zinatizadeh and M.C. Van Loosdrecht. 2021. A comprehensive comparison between biochar and activated carbon for contaminants adsorption: a review. Environmental Science and Pollution Research. 28:35874-35906.

Aweto, K. E., & Ovwamuedo, G. (2023). Simulation of contaminants transport from a dumpsite into shallow aquifer of the upper deltaic plain deposits, Western Niger Delta. Journal of Scientific Research, 15(2), 301-312.

Carolin, C.F. and P.S. Kumar, A. Saravanan, G.J. Joshiba and M. Naushad. 2017. Efficient techniques for the removal of toxic heavy metals from aquatic environment: a review. Journal of Environmental Chemical Engineering. 5:2782-2799.

Chen, Y.D., S.H. Ho, D. Wang, Z.S. Wei, J.S. Chang and N.Q. Ren. 2018. Lead removal by a magnetic biochar derived from persulfate-zvi treated sludge together with one-pot pyrolysis. Bioresource Technology. 247:463-470.

Cho, C. H., & as-, U. O. T. A. A. I. A. (2004). Why do people avoid advertising on the internet?. Journal of advertising, 33(4), 89-97.

Duan, W., J. Li, Y. Chen, L. Wang, Y. Wang, L. Wang, Y. Zhao and Z. Li. 2020. Enhanced immobilization of heavy metals in wastewater using biochar-supported nano-Zn° composites. Environmental Research. 182:109-120.

Fei, Y. and Y.H. Hu. 2022. Design, synthesis, and performance of adsorbents for heavy metal removal from wastewater: a review. Journal of Materials Chemistry. 10:1047-1085.

Foo, K.Y. and B.H. Hameed. 2010. Insights into the modeling of adsorption isotherm systems. Chemical Engineering Journal. 156:2-10.

Ghandali, M.V., S. Safarzadeh, R. Ghasemi-Fasaei and S. Zeinali. 2024. Heavy metals immobilization and bioavailability in multi-metal contaminated soil under ryegrass cultivation as affected by ZnO and MnO2 nanoparticle-modified biochar. Scientific Reports. 14:10684-10695.

Ho, Y.S. and G. McKay. 1999. Pseudo-second order model for sorption processes. Process Biochemistry. 34:451-465.

Inyang, M.I., B. Gao, Y. Yao, Y. Xue, A. Zimmerman, A. Mosa, P. Pullammanappallil, Y.S. Ok and X. Cao. 2016. A review of biochar as a low-cost adsorbent for aqueous heavy metal removal. Critical Reviews in Environmental Science and Technology. 46:406-433.

Jha, P.K. and P. Tripathi. 2021. Arsenic and fluoride contamination in groundwater: A review of global scenarios with special reference to india. Groundwater for Sustainable Development. 13:576-590.

Kanmani, S., & Gandhimathi, R. (2013). Assessment of heavy metal contamination in soil due to leachate migration from an open dumping site. Applied water science, 3(1), 193-205.

Khanzada, Z.T., S.R. Naqvi, I. Ali, A.E. Atabani, M.N. Anjum, A.S. Nizami, M. Rehan, M. Shahbaz and S. Minahal. 2023. Recent advances in hydrochar application for the adsorptive removal of wastewater pollutants. Chemical Engineering Communications. 210:200-222.

Krishnakumari, A., Devaraju, A., & Saravanan, M. (2018). Evaluation of mechanical properties of hybrid rootfiber reinforced polymer composites. Materials Today: Proceedings, 5(6), 14560-14566.

Lapworth, D. J., Krishan, G., MacDonald, A. M., & Rao, M. S. (2017). Groundwater quality in the alluvial aquifer system of northwest India: new evidence of the extent of anthropogenic and geogenic contamination. Science of the total Environment, 599, 1433-1444.

Lee, S., & Heo, C. Y. (2009). Corporate social responsibility and customer satisfaction among US publicly traded hotels and restaurants. International Journal of Hospitality Management, 28(4), 635-637.

Levin, E. G., Lustig, Y., Cohen, C., Fluss, R., Indenbaum, V., Amit, S., ... & Regev-Yochay, G. (2021). Waning immune humoral response to BNT162b2 Covid-19 vaccine over 6 months. New England Journal of Medicine, 385(24), e84.

Li, X., C. Wang, Y. Zhang and M. Liu. 2023. Nano-modified biochar for enhanced environmental remediation: Synthesis, characterization and applications. Science of the Total Environment. 856:159234-159247.

Liu, Z., Z. Xu, L. Xu, F. Buyong, T.C. Chay, Z. Li, Y. Cai, B. Hu, Y. Zhu and X. Wang. 2022. Modified biochar: synthesis and mechanism for removal of environmental heavy metals. Carbon Research. 1:8-18.

Macedo, S., Gomes, J., Quinta-Ferreira, R.M. and Martins, R.C. 2021. Application of thiourea-modified biochar for cadmium removal from synthetic wastewater. Water Science and Technology. 84:89-101.

Ouyang, Y., Zhu, W., Yao, X., Ye, C., Lei, B., Rong, X., Zheng, J., Liu, X., Wu, J., Liu, X. and Ding, C. 2024. ZnCl2 and thiourea co-modified biochar for effectively removing quinclorac in water and soil: Mechanism and alleviating its phytotoxicity on tobacco plants. Separation and Purification Technology. 350:127-230.

Phiri, Z., N.T. Moja, T.T. Nkambule and L.A. de Kock. 2024. Utilization of biochar for remediation of heavy metals in aqueous environments: A review and bibliometric analysis. Heliyon. 10:145-162.

Rahman, Z. and V.P. Singh. 2019. The relative impact of toxic heavy metals (thms)(arsenic (as), cadmium (cd), chromium (cr)(vi), mercury (hg), and lead (pb)) on the total environment: An overview. Environmental monitoring and assessment 191:1-21.

Saleh, T.A. 2024. Nanomaterials for water treatment: Synthesis, applications, and environmental impacts. Chemosphere. 356:141876.

Shaheen, S.M., A. Mosa, Natasha, H. Abdelrahman, N.K. Niazi, V. Antoniadis, M. Shahid, H. Song, E.E. Kwon and J. Rinklebe. 2022. Removal of toxic elements from aqueous environments using nano zero-valent iron-and iron oxide-modified biochar: a review. Biochar. 4:24-41.

Singh, P., Kumar, A., Sharma, R. and Gupta, N. 2023. Optimization of sorbent dosage for nano-modified biochar in heavy metal removal applications. Water, Air, and Soil Pollution. 234:189.

Wang, S., B. Gao, A.R. Zimmerman, Y. Li, L. Ma, W.G. Harris and K.W. Migliaccio. 2019. Removal of arsenic by magnetic biochar prepared from pinewood and natural hematite. Bioresource Technology. 175:391-395.

Zhang, M., Y.G. Liu, T.T. Li, W.H. Xu, B.H. Zheng, X.F. Tan, H. Wang, Y.M. Guo, F.Y. Guo and S.F. Wang. 2022. Chitosan modification of magnetic biochar produced from Eichhornia crassipes for enhanced sorption of Cr(VI) from aqueous solution. RSC Advances. 5:46955-46964.

Zhu, R., Q. Chen, Q. Zhou, L. Wang, Y. Sun, L. Pan and X. Zhang. 2020. Thiourea-modified biochar for efficient heavy metal removal from wastewater. Bioresource Technology. 306:123-140.

Zhu, S., X. Huang, D. Wang, L. Wang and F. Ma. 2020. Enhanced hexavalent chromium removal performance and stabilization by magnetic biochar composite: effects of pyrolysis temperature and particle size. Environmental Pollution. 260:114021.